Characterization and Preparation of Polyion Complex Composite Membranes for the Separation of Methyl *tert*-Butyl Ether/Methanol Mixtures

SANG-GYUN KIM,[1] YONG-IL KIM,[1] JONGGEON JEGAL,[1] GYUN-TAEK LIM,[2] KEW-HO LEE[1]

[1] Membrane and Separation Research Center, KRICT, P.O. Box 107, Yusung, Taejon 305-606, South Korea

[2] Department of Polymer Engineering, Chonnam National University, Gwangju 500-757, South Korea

Received 13 December 2000; accepted 8 October 2001

ABSTRACT: A series of polyion complex (PIC) composite membranes composed of sodium alginate (SA) polyanion and chitosan polycation were prepared by varying the ratio of concentration. The interaction between SA and chitosan was investigated by FTIR, SEM, and X-ray analysis and was related to mechanical properties and the swelling phenomenon. The overall PIC composite membranes showed the following results: the total thickness of the coating layer was thicker than that of pure SA composite, and increased with increasing the concentration of chitosan solution during PIC formation. This result was attributed to the diffusion of chitosan molecules from the liquid solution into the SA matrix, and the incorporation with SA molecules. For the PIC membranes prepared with different concentrations of polymer solution, their structural differences could not be detected from IR spectra but their morphological differences could be noticeably found from SEM. Furthermore, the amorphousness of PIC membranes and their elongation properties at break increased significantly as a function of polymer contents, whereas the tensile modulus decreased because of the physical transition effect. © 2002 Wiley Periodicals, Inc. J Appl Polym Sci 85: 714–725, 2002

Key words: sodium alginate; chitosan; pervaporation; MTBE/methanol mixture

INTRODUCTION

Pervaporation is a technique to separate a mixture of liquids by membranes. Numerous membranes were prepared and used for the separation of organic mixtures by pervaporation.[1] The simultaneous enhancement of both parameters, however, has been a big challenge because of the trade-off phenomenon between flux and separation factor that is frequently encountered in pervaporation experiments. Therefore, to prepare the membranes having a high permeability and a high separation capability, many polymer membranes were investigated and, among the hydrophilic polysaccharide-type polymers, ionomers such as alginate and chitosan have gained special interest because they showed the highest flux and separation factor for the pervaporation dehydration. In particular, the separation of an organic mixture using a polyelectrolytes complex has focused on one of the membrane materials because of its high chemical stability as well as hydrophilicity attributed to its ionic complex. For the separation of water and ethanol mixtures by pervaporation, these membranes exhibit high permselectivity for the water component.[2,3]

The separation of polar/nonpolar organic mixtures such as methyl *tert*-butyl ether (MTBE)/methanol and benzene/cyclohexane mixtures by

Correspondence to: S.-G. Kim (khlee@ krict.re.kr).

Journal of Applied Polymer Science, Vol. 85, 714–725 (2002)

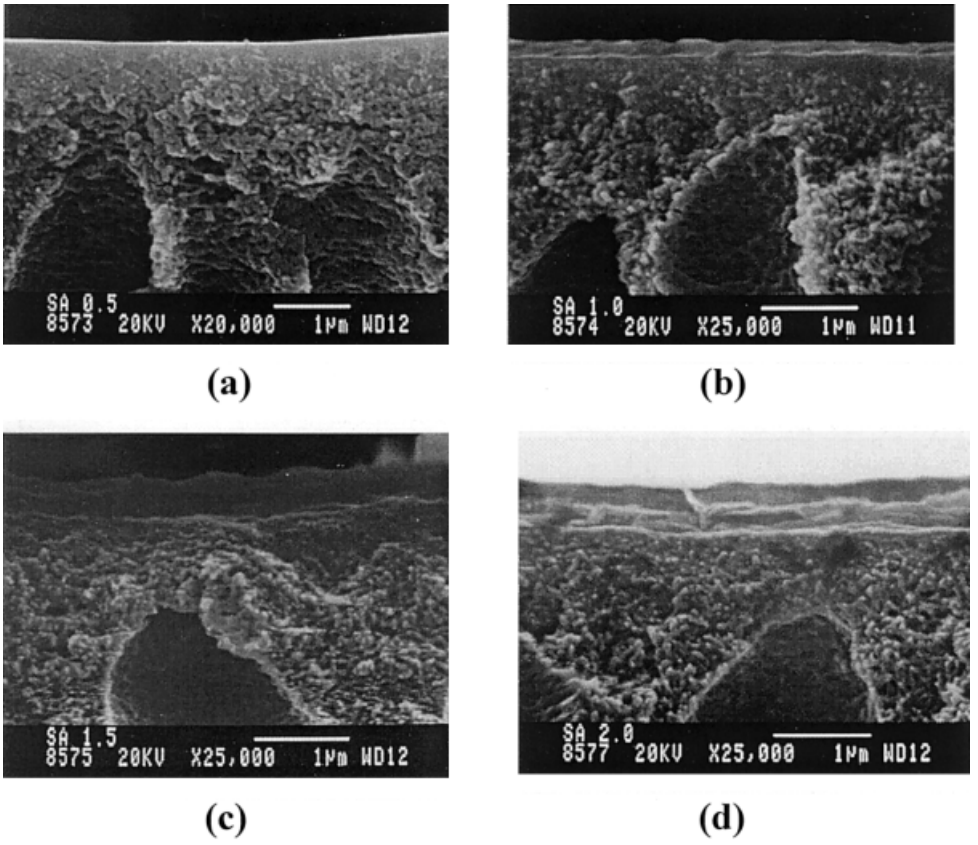

Figure 1 SEM micrographs of SA composite membranes, prepared at different contents of SA: (a) 0.5%; (b) 1.0%; (c) 1.5%; (d) 2.0%.

pervaporation membranes was the focus of a recent investigation.[4] However, the highly effective pervaporation membranes for the separation of organic/organic mixtures have not yet been developed. In this study, to develop the high-performance membranes for the separation of polar and nonpolar organic mixtures, polyion complex (PIC) composite membranes composed of sodium alginate (SA) as polyanion and chitosan as polycation were investigated. Although studies on the complexation between SA and chitosan had already been reported, it was interesting to investigate the formation of composite membranes utilizing the unique properties of SA and chitosan. The layer-by-layer interfacial reaction of polycationic and polyanionic components was considered on a microporous support membrane for the formation of the PIC composite membrane.[5,6] These PIC composite membranes showed very high performance for the pervaporation separation of MTBE/methanol mixtures. Therefore, the aim of this work was to characterize PIC composite membranes prepared by interfacial reaction of polyanion and polycation, used at various concentrations, to better understand their structures and separation behaviors. For this purpose, the morphology and the chemical structure of membranes were studied using FTIR, X-ray, and SEM analyses, whereas the tensile strength was tested to investigate the modulus of membranes and their elongation behavior. The characteristics of PIC composite membrane are discussed from the viewpoint of membrane preparation conditions.

EXPERIMENTAL

Materials

Sodium alginate (SA), methyl *tert*-butyl ether (MTBE), and chitosan were purchased from Aldrich Chemicals (Milwaukee, WI). Polysulfone membrane (MWCO 30,000) for the supporters of composite membranes was purchased from U.O.P. Corp. (San Diego, CA). Methanol (guaranteed reagent) was supplied by Merck (Darmstadt,

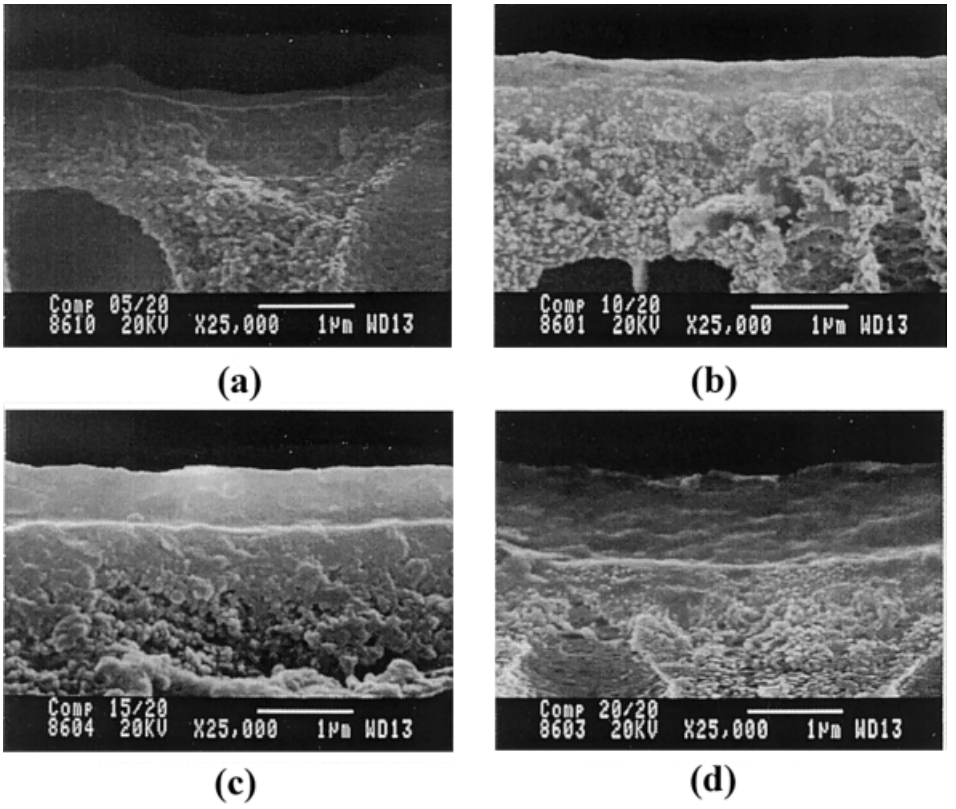

Figure 2 SEM micrographs of PIC composite membranes, prepared at different SA contents, in a 2.0% chitosan solution: (a) 0.5%; (b) 1.0%; (c) 1.5%; (d) 2.0%.

Germany). HCl (35% content, extrapure grade) and ethanol (guaranteed reagent) were purchased from Junsei Chemical Co. (Tokyo, Japan). Ultrapure deionized water was used. All chemicals were used without any further purification.

Membrane Preparation

SA solutions of 0.5–2.0 wt % concentrations were prepared by dissolving SA in water. To prepare the composite-type polyion complex membranes, pure SA composite membranes were first prepared by dipping the skin layer side of polysulfone membranes into each SA solution and drying them at room temperature in a fume hood for 1 day. Chitosan solutions of 0.5–2.0 wt % concentrations were prepared by dissolving chitosan in water containing 5 wt % of HCl. The prepared, pure SA composite membranes were then immersed in a chitosan solution for 10 min. After the polyion complexation, the membrane was taken out of the chitosan solution, washed several times with pure water to eliminate any possible residual chitosan solution, and dried at room temperature.

Membrane Characterization

Infrared Measurement of Prepared PIC Membranes

The chemical structures of the prepared PIC membranes were characterized by a Fourier transform infrared spectroscopy (Digilab FTS-80; Bio-Rad, Richmond, CA).

X-ray Differential Observation

The change of membrane structure, under different polyion complexation conditions, was investigated by wide-angle X-ray diffractometry (model D/MAX IIIB; Rigaku, Japan) with a scintillation counter detector, using CuK_{α} radiation as a source. Scans of Bragg's angle 2θ ranged from 2ϕ to 50°.

Scanning Electron Microscopy (SEM)

The surface morphologies and internal structures of the PIC membranes were examined using a JEOL JSM-80A scanning electron microscope (JEOL, Peabody, MA). For this SEM study, mem-

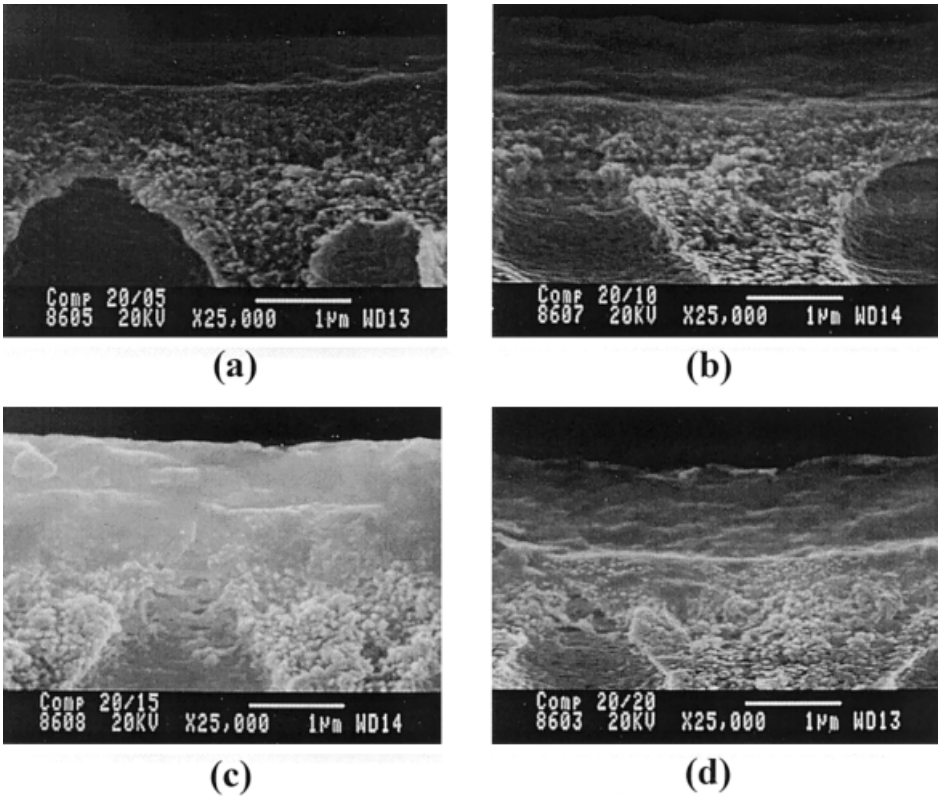

Figure 3 SEM micrographs of PIC composite membranes, prepared at different chitosan contents, for 2.0% SA membrane: (a) 0.5%; (b) 1.0%; (c) 1.5%; (d) 2.0%.

brane samples were fractured in liquid nitrogen and coated with gold.

Mechanical Properties

Strip specimens ($60 \times 80 \times 0.2$ mm^3) of dried films were used to test their tensile strengths with a strain rate of 10 mm min^{-1}, on a Shimadzu Autograph stress-strain testing machine (Model AGS-500D, Japan), at 25°C.

Swelling Ratio

The dried membranes were cut into fragments of about 20–25 mg. These fragments were weighed accurately and kept in a closed chamber saturated with MTBE/methanol mixtures at 40°C. The uptake W_s was calculated by measuring the weight gain of the sample at different times, after carefully wiping the surface with a filter paper. The swelling ratio S was obtained from the weights of a sample in the dry state and in the swollen state, according to

$$S = (W_s - W_d)/W_d$$

where W_d and W_s indicate the weight of the dry and the swollen membranes, respectively.

RESULTS AND DISCUSSION

Morphology of Prepared Membranes

Scanning electron micrographs of both surface segments and cross sections of SA and PIC-composite membranes are shown in Figures 1–4, respectively. As can be seen in Figures 2 and 3, the overall PIC composite membranes clearly show that the total thickness of the coating layer was thicker than not only that of pure SA composite, but also that of membranes increased with increasing the concentration of chitosan solution in the polyion complexation reaction between SA and chitosan. Furthermore, in Figure 4, with the increase of complexation time from 10 min to 24 h, the active layer grew thicker. The results of these investigations are summarized in Table I. From this observation, it can be considered that PIC membrane formation between SA polyanion

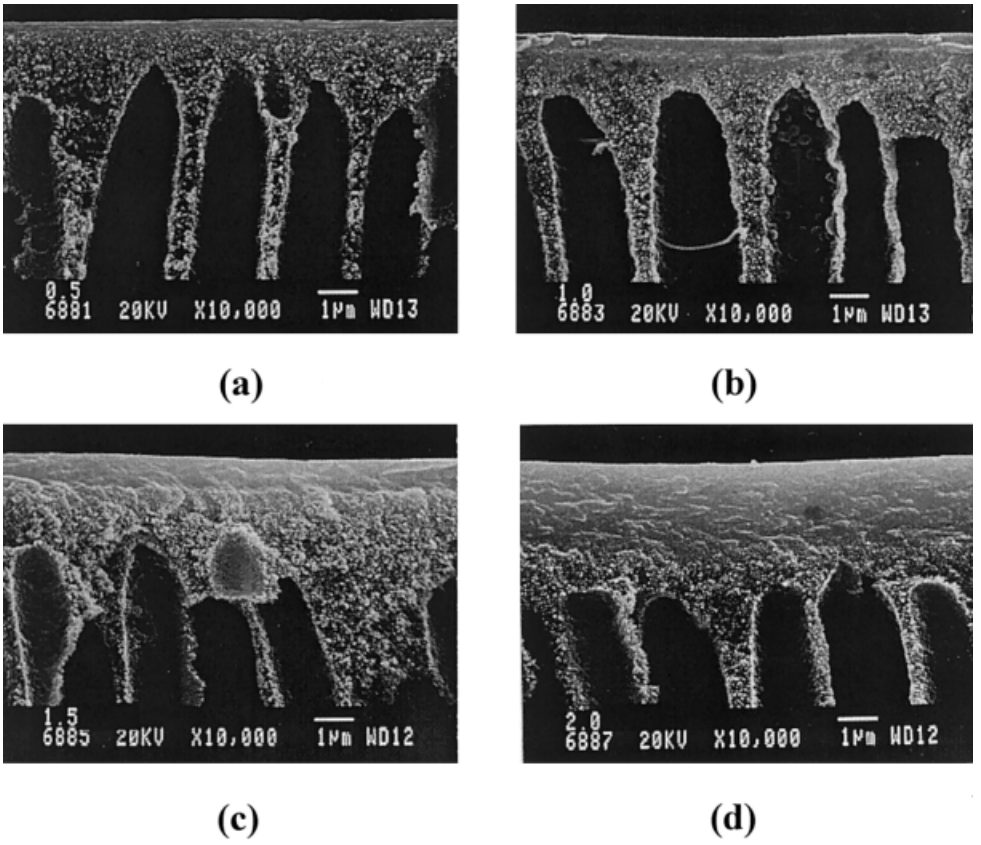

Figure 4 Effect of complexation time on the PIC composite membranes, prepared at different SA contents, in a 2.0% chitosan solution: (a) 0.5%; (b) 1.0%; (c) 1.5%; (d) 2.0%.

and chitosan polycation is attributable to the layer-by-layer assembly of oppositely charged polymers on solid surfaces, which corresponds to the results of both Decher's and Stoeve's investigative groups.[5,6] The thickness variation of the active layer of cationic and anionic polymers on porous supporting membranes highly depended on the chitosan and SA content in the dipping solution during PIC membrane formation.

Table I Thickness of the Coating Layer of SA and PIC Composite Membranes

Membrane Type	Coating Layer Thickness (μm)
0.5% SA	0.07
1.0% SA	0.19
1.5% SA	0.48
2.0% SA	0.60
0.5 SA/2.0 CH	0.18
1.0 SA/2.0 CH	0.43
1.5 SA/2.0 CH	0.70
2.0 SA/2.0 CH	1.15
2.0 SA/0.5 CH	0.53
2.0 SA/1.0 CH	0.94
2.0 SA/1.5 CH	0.81
2.0 SA/2.0 CH	1.15

To observe the morphology change during polyion complexation, the cross-sectional views of homogeneous pure membranes and the polyion-complexed membranes of SA and chitosan were investigated and are shown in Figures 5, 6, and 7. In the case of pure SA membranes, the particle phase is shown at a magnification of $\times$10,000, and with the increase of SA content, the distribution of particles decreased. This type of morphology also appeared in the complexed membranes, although the size of the particle phase was smaller than that shown in pure SA membranes and the structure of membranes was varied somewhat. The particle-like phase observed in pure SA membranes seems like the gel structure derived from the solution state. That is, the physical properties of polysaccharides such as SA are largely determined by interactions of their chemical structure with the surrounding ionic environment. The large molecular weight (over 100

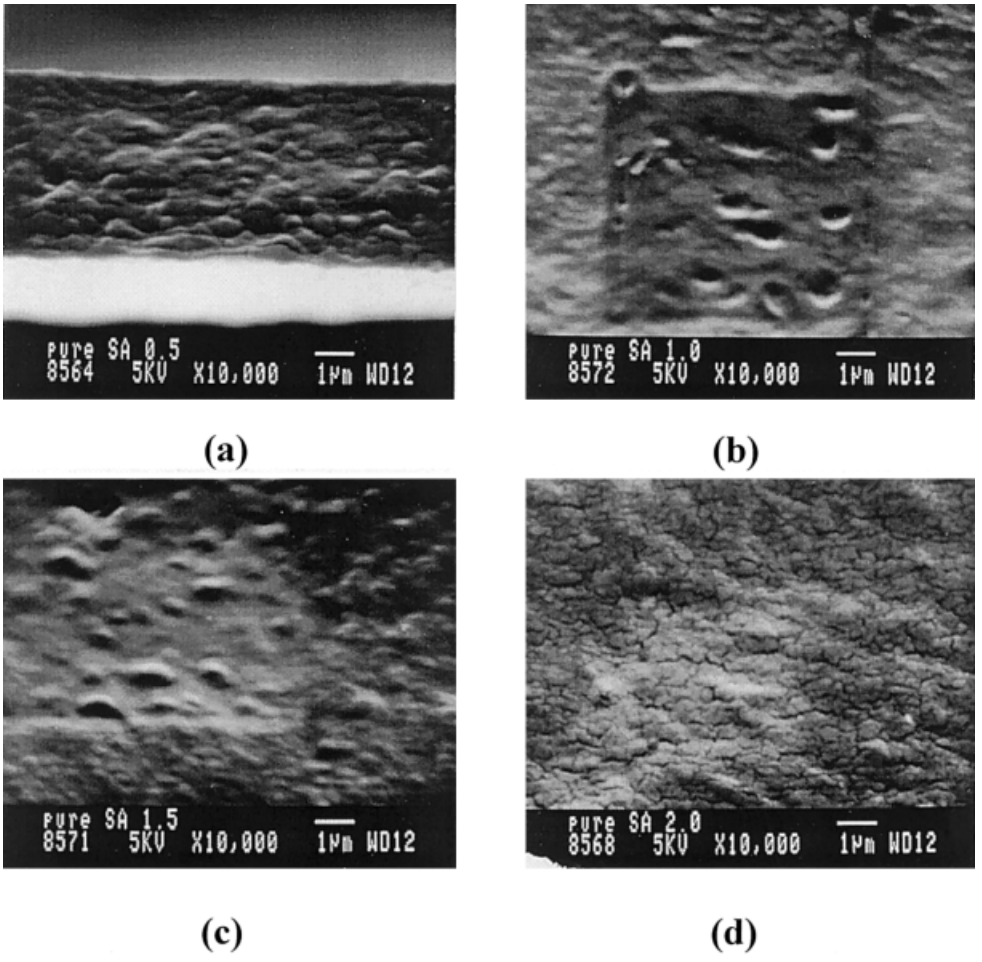

Figure 5 SEM micrographs of pure SA membranes: (a) 0.5%; (b) 1.0%; (c) 1.5%; (d) 2.0%.

kDa) and anionic nature of polysaccharide allow these molecules to exist in a continuum of physical states, ranging from dense gels to dilute solutions. Generally, SA is a heteropolymer of greater than 130 kDa in size, composed of two ionic monomer units: (1→4)-linked α-L-guluranate (G) and (1→4)-linked β-D-mannuronate (M). The residues are arranged in irregular blocks along a linear chain.[7] Accordingly, as can be seen from Figure 5, pure SA membranes have most of the particles of 1 μm size and show the particle-like phase distribution as a function of SA content, respectively. On the order hand, when these membranes are complexed with chitosan, as can be seen from Figures 6 and 7, the overall particle phase is reduced both in size and in number. Particularly in the case of 2.0% SA/2.0% chitosan, and 2.0% SA/1.5% chitosan complexed composition, the particles disappeared and SEM showed the morphologies in the form of a strand. Based on these figures, when the chitosan molecules diffuse into SA membranes and two polymers are complexed, two occurrences can be considered. First of all, the SA particles that are formed are able to disentangle the several polymer molecules arranged as an aggregate as a result of the effect of the interphasic structure formation by the interaction of the anionic SA with the cationic chitosan. Second, we can see that at the higher concentration of polymer, the physical transition phenomenon of particles facilitates. From the above-mentioned results, it was considered that the chitosan molecules diffuse from the liquid solution into the SA matrix and incorporate with SA molecules.

FTIR Spectra

In principle, SA is a polysaccharide consisting of linear chains of 1→4-linked β-D-mannuronate (M) and α-L-guluronate (G) residues in various proportions and arranged in blocks of the two mono-

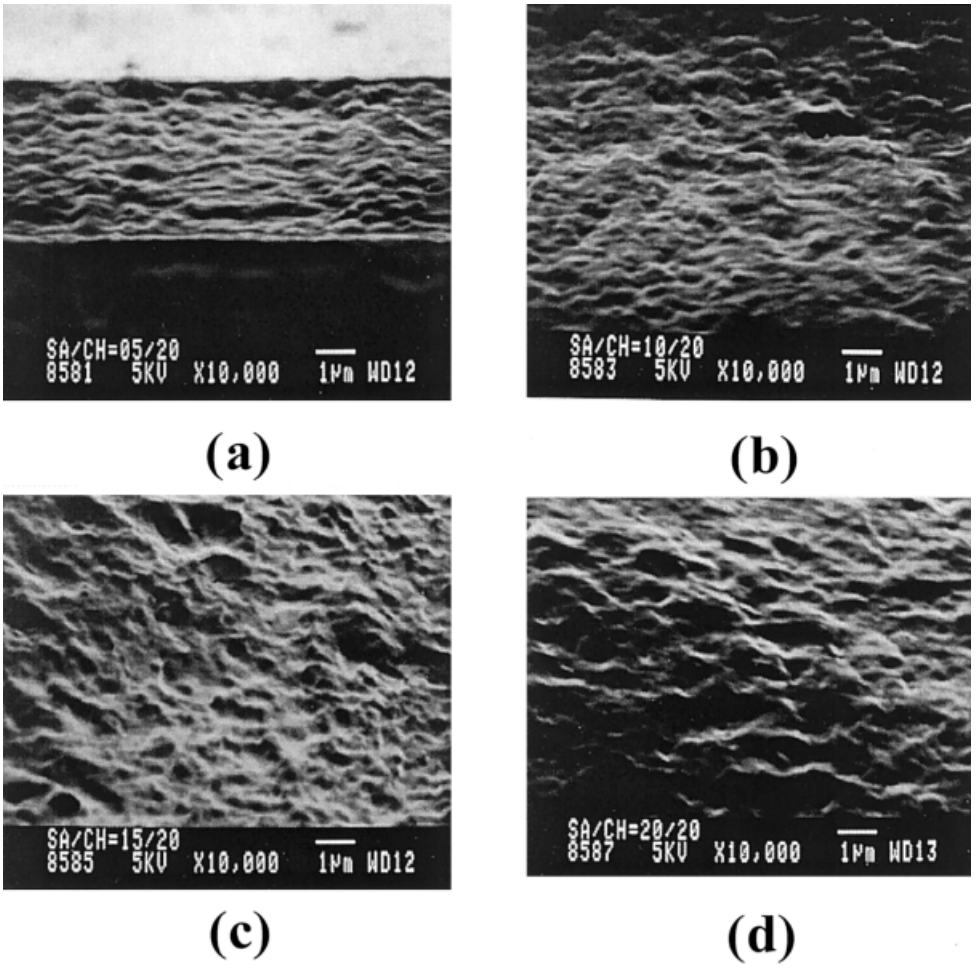

Figure 6 SEM micrographs for the cross sections of PIC membranes, prepared at different SA contents, in a 2.0% chitosan solution: (a) 0.5 SA/2.0 chitosan; (b) 1.0 SA/2.0 chitosan; (c) 1.5 SA/2.0 chitosan; (d) 2.0 SA/2.0 chitosan.

mers,[8] whereas chitosan is composed of 1→4-linked 2-amino-2-deoxy-β-D-glucan and is prepared by N-deacetylation of chitin.[9] The cation-charged chitosan could be complexed by carboxylate groups of SA in a tetra-dentate structure (the well-known egg-box model).[10] Figures 8 and 9 show the IR spectra of chitosan, SA membrane, and PIC membranes, prepared by varying the ratios of concentration. First, as can be seen from Figure 8, chitosan[11] is characterized by its saccharide structure bands at 902 and 1155 cm^{-1}, an amino band at 1587 cm^{-1}, and an amide 1 band of the acetyl group at 1651 cm^{-1}. The IR spectrum of SA[12] showed COO^- asymmetric and symmetric stretching peaks of carboxylate salts groups at 1620 and 1416 cm^{-1}. In the case of PIC membrane, new bands observed at 1736 and 1242 cm^{-1} were attributed to the asymmetric and symmetric stretching of COO^- groups, respectively. The band appearing at 1639 cm^{-1} in the spectrum of polyion complex membranes can be assigned to a symmetric NH_3^+ deformation, and broad bands appearing at 2500 and 1900 cm^{-1} confirm the presence of NH_3^+ on the polyion complex membrane.[13] Moreover, as the polyion complex formation proceeds, at 3380 cm^{-1} the O—H stretching peak becomes narrower and exhibits not only a small shift to higher wavenumbers but also a decrease in intensity. This phenomenon also would be expected because of an increase in intermolecular interaction, such as hydrogen bonding between SA and chitosan. These results imply that the carboxylate groups of SA were dissociated to COO^- groups that complexed with protonated amino groups from chitosan through electro-

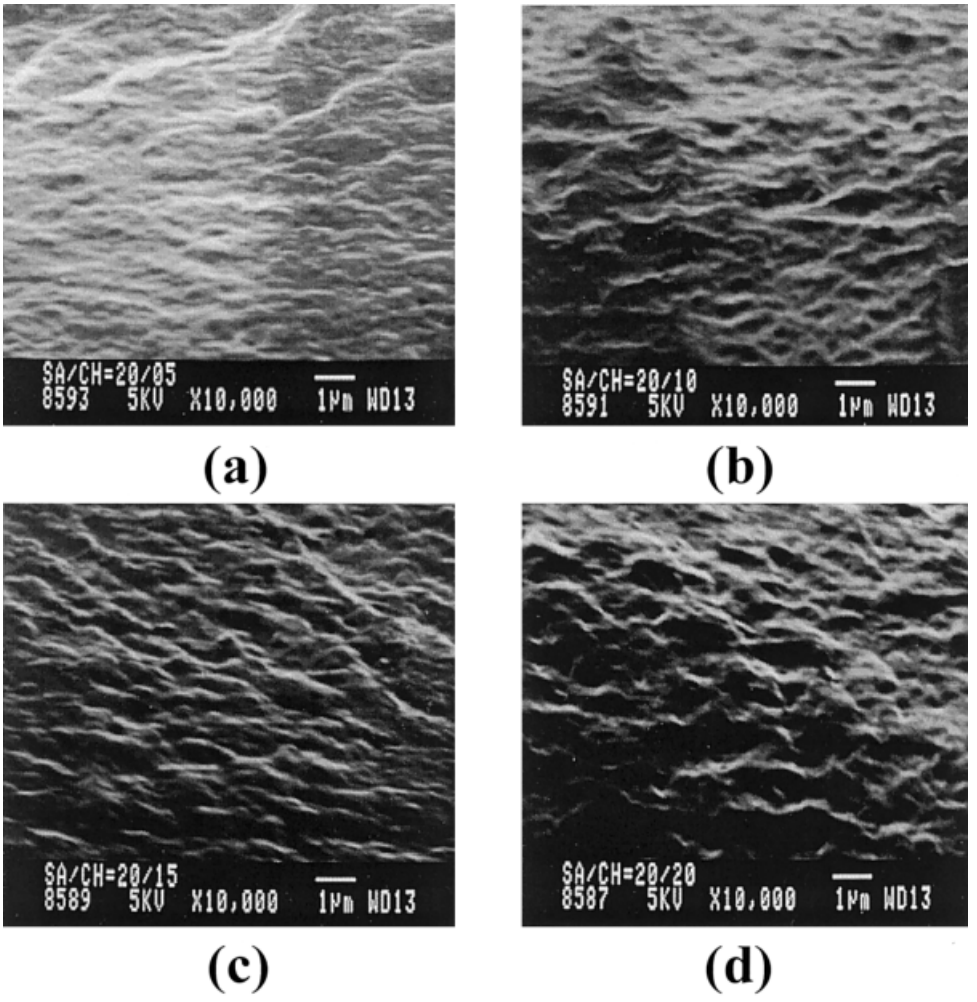

Figure 7 SEM micrographs for the cross sections of PIC membranes, prepared at different chitosan contents, for 2.0% SA membrane: (a) 2.0 SA/0.5 chitosan; (b) 2.0 SA/1.0 chitosan; (c) 2.0 SA/1.5 chitosan; (d) 2.0 SA/2.0 chitosan.

static interaction during polyion complex formation.

In the case of PIC membranes prepared with different SA concentrations, however, the structural changes obviously could not be found from the IR spectrum. According to these results, it is considered that the concentration of SA and chitosan solution in the complexation does not cause any significant effect in the chemical structure, which means that the diffusion surroundings of chitosan molecules that penetrated into the SA membranes are similar to each other. This indicates that the morphology of PIC membranes depends strongly on the physical transition states of pure SA membranes, and the overall structure of these membranes can be affected by electrostatic interactions that occur between the particles in the SA membranes and the chitosan molecules. In addition, to consider the relation between the diffusion of chitosan molecules and the intensity of complexation, the structural changes at the polymer composition of 2.0% SA/2.0% chitosan were investigated as a function of time. As can be seen in Figure 10, the time variation did not cause any notable change on the degree of PIC, given that the complexation rate by diffusion of chitosan molecules into the SA membrane was very fast. From the above result, it was concluded that the chitosan penetration and complexation with SA occurred simultaneously. On the other hand, in the case of PIC membranes prepared with different chitosan solutions, the degree of polyion complexation increased with increasing the concentration of chitosan solution, as shown in Figure 9.

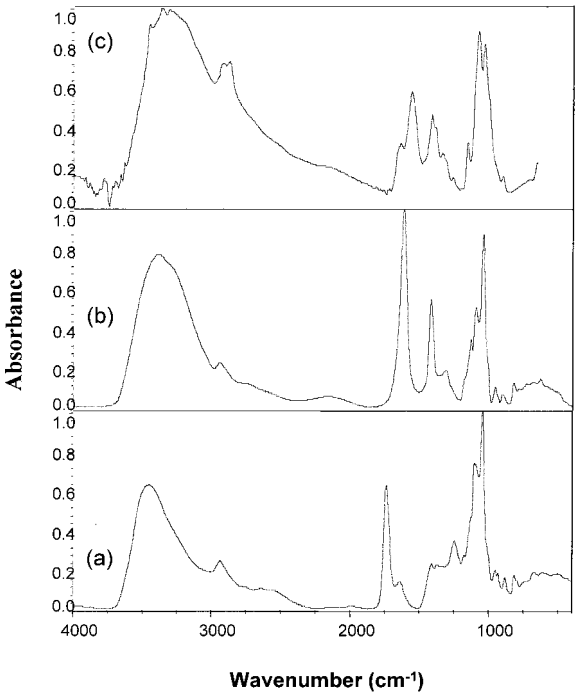

Figure 8 FTIR spectra of the prepared membranes: (a) chitosan; (b) sodium alginate; (c) polyion complex membrane.

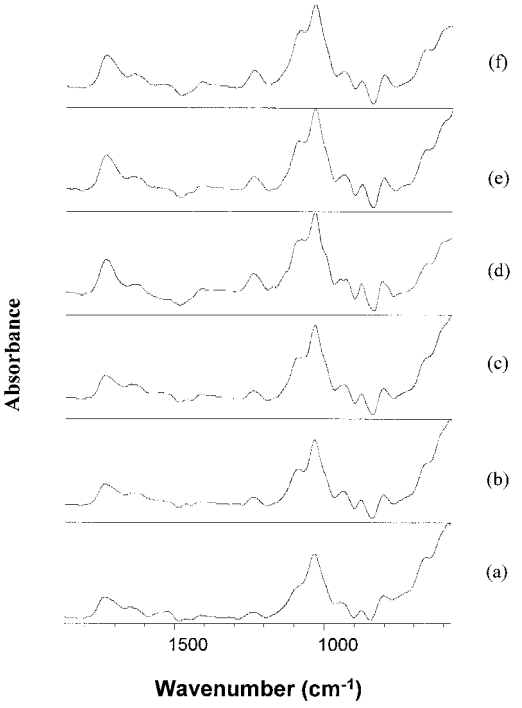

Figure 10 Effect of complexation time on the FTIR spectra of the PIC membranes: (a) 30 s; (b) 1 min; (c) 5 min; (d) 10 min; (e) 30 min; (f) 14 h.

X-ray Diffraction Patterns

In Figure 11, the XRD results obtained from SA, chitosan, and PIC membranes are shown. SA showed an almost entirely amorphous morphology, whereas chitosan exhibited a semicrystalline characteristic having a typical peak at 2θ values of 10 and 20°, respectively.[14] However, polyion complex, formed by electrostatic interaction between SA and chitosan, showed the increase of the amorphous state significantly more than that of SA, and a crystalline peak of chitosan at $2\theta = 10°$ [Fig. 11 (c)] disappeared. Particularly, the reason for the deformation of crystal structure could be explained in terms of the break of hydrogen bonding between amino groups and hydroxyl groups in the chitosan, resulting from complexation.[15] In Figure 12, X-ray patterns of PIC mem-

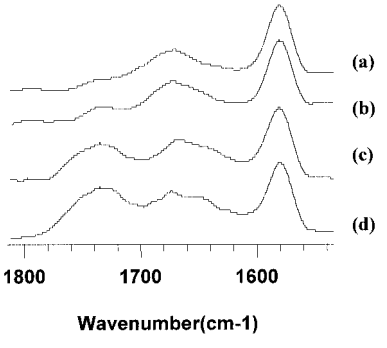

Figure 9 FTIR spectra of the PIC membranes, prepared with different chitosan solutions: (a) 2.0 SA/0.5 chitosan; (b) 2.0 SA/1.0 chitosan; (c) 2.0 SA/1.5 chitosan; (d) 2.0 SA/2.0 chitosan.

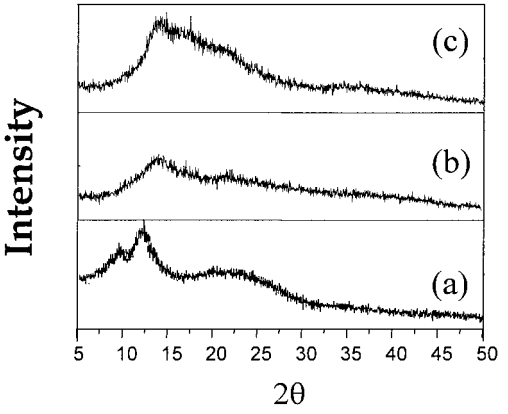

Figure 11 X-ray diffraction patterns of the PIC membranes: (a) chitosan; (b) SA; (c) polyion complex membrane.

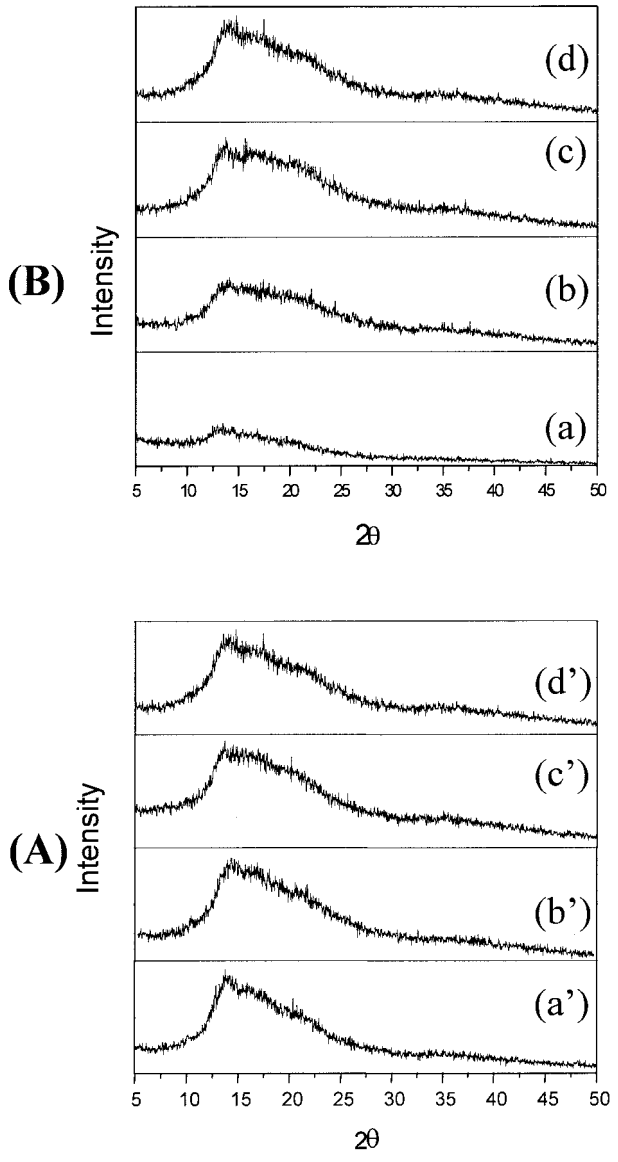

Figure 12 X-ray diffraction patterns of the PIC membranes, prepared with different polymer contents. (A) Membranes prepared with different chitosan solutions: (a′) 2.0 SA/0.5 chitosan; (b′) 2.0 SA/1.0 chitosan; (c′) 2.0 SA/1.5 chitosan; (d′) 2.0 SA/2.0 chitosan. (B) Membranes prepared with different SA contents: (a) 0.5 SA/2.0 chitosan; (b) 1.0 SA/2.0 chitosan; (c) 1.5 SA/2.0 chitosan; (d) 2.0 SA/2.0 chitosan.

branes with different polymer contents are shown. With increasing SA content, the overall amorphous characteristics of PIC membranes obviously increased, but with different chitosan solutions these morphological changes were scarcely observed. Consequently, we have to assume that when the physical transitions of SA membranes are identical, the structural characteristics show a similar status, whereas the structure of these membranes varies if the physical transition is obviously different. In addition, Figure 13 shows the correlation between the morphological change and complexation time. The amorphous status of these membranes during PIC formation is not largely increased by the complexation time, but it is obvious that the morphology is somewhat influenced by the complexation time, as shown by the SEM results of Figure 7.

Mechanical Properties

Tensile modulus and elongation at break for PIC membranes are shown in Figure 14. Introducing rigid chitosan molecules into the SA matrix increased their elongation at break compared with that of pure SA membranes as a function of polymer contents, whereas it decreased the tensile modulus. Furthermore, the physical transition phenomenon, as shown in Figures 8 and 9, by complexation between two polymers was accompanied by an increase of elongation of PIC compared with that of the pure SA membranes. These

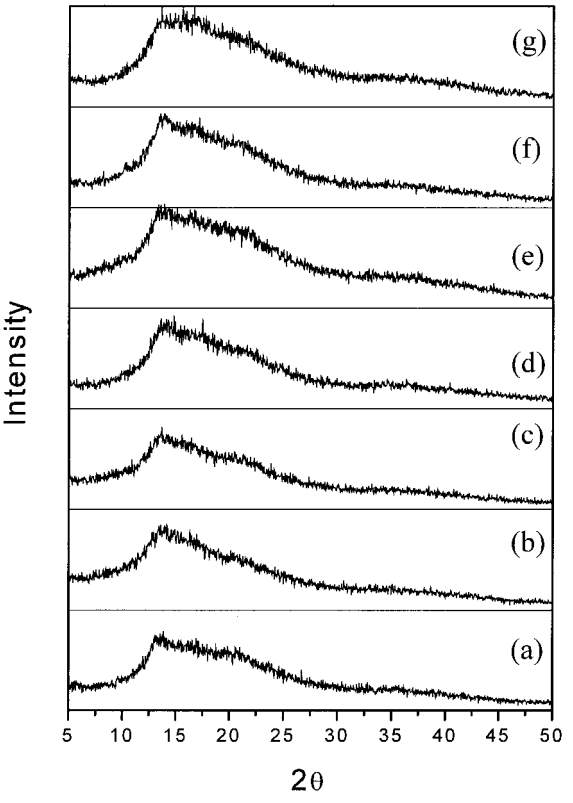

Figure 13 Effect of complexation time on the X-ray diffraction patterns of the PIC membranes: (a) 30 s; (b) 1 min; (c) 5 min; (d) 10 min; (e) 30 min; (f) 14 h; (g) 48 h.

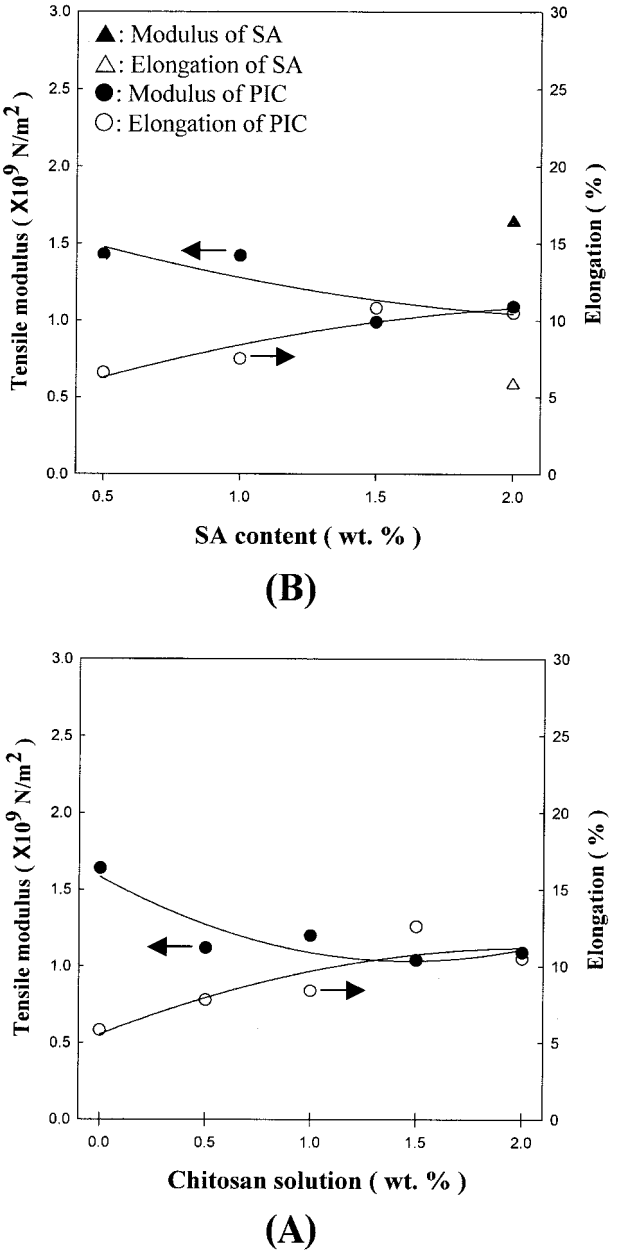

Figure 14 Modulus and elongation of the PIC membranes, prepared with different polymer contents: (a) membranes prepared with different chitosan solutions; (b) membranes prepared with different SA contents.

results of elongation correspond to the changes of the X-ray patterns of Figure 12. Moreover, it shows that the increase of elongation properties is attributable to the increase of amorphous properties of PIC.

Swelling Properties

To clarify the correlation between swelling and complexation, the equilibrium/swelling ratio for the MTBE and methanol mixtures was investigated. As shown in Figure 15, the degree of swelling of the PIC membranes prepared with different SA contents increased as a function of SA content, whereas that of PIC membranes made from dif-

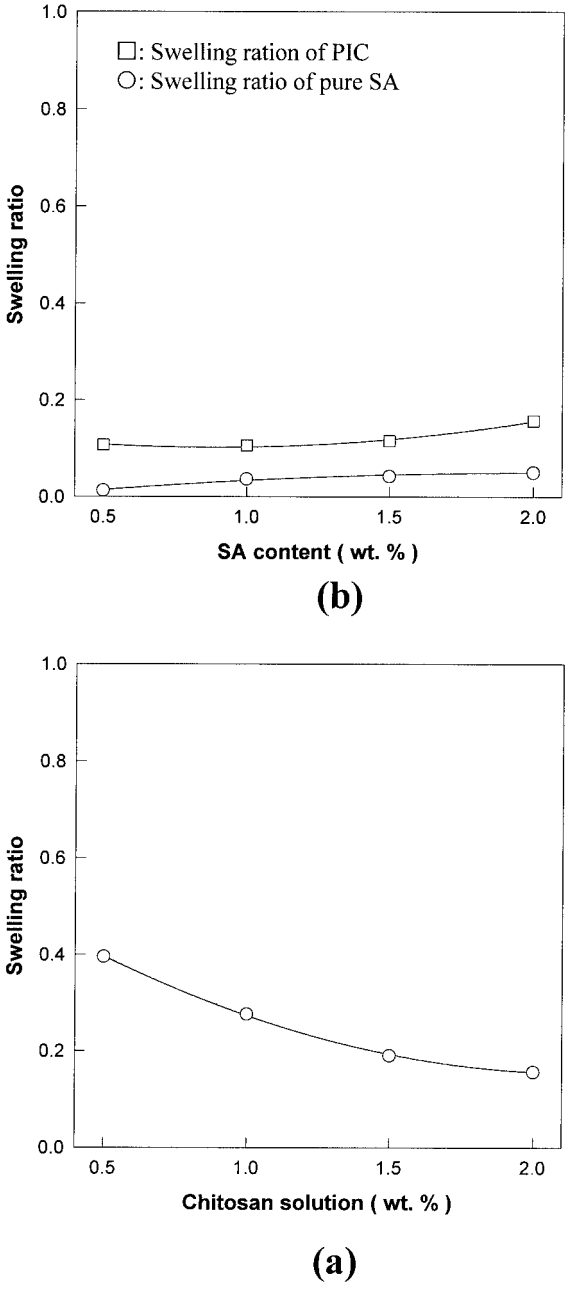

Figure 15 Swelling ratio of the pure SA and PIC membranes, prepared with different polymer contents, in a 75 wt % MTBE solution at 40°C: (a) PIC membranes, prepared with different chitosan solutions; (b) swelling ratio of the pure SA and PIC membranes, prepared with different SA contents.

ferent chitosan solutions decreased by increasing the concentration of chitosan. However, the differences of swelling ratio of the membranes were small. The thickness of the membrane increased with the concentration of chitosan solution during PIC formation, and the influence of SA content in dipping solutions on the resulting membrane thickness was also shown. Therefore, the swelling behavior of pure SA membranes is explained by the affinity of SA toward methanol molecules; that is, by increasing the thickness of SA membranes, the swelling ratios increase because of an increase of the amount of adsorbed methanol. Accordingly, for the PIC membrane prepared as a function of SA contents, the swelling result is mainly attributed to the SA thickness in the PIC membranes, whereas in the case of the same content of SA, the swelling characteristic is considered to be attributable to the structural changes by electrostatic interaction between SA and chitosan. In principle, a polymeric material with higher crosslinked density has a lesser membrane mobility and a more compact network structure, resulting in a lower swelling ratio. In the same way, the swelling ratio increases with reduced chitosan concentration during PIC formation.

CONCLUSIONS

To prepare the polyion complex (PIC) composite membranes composed of sodium alginate (SA) and chitosan, the complexation phenomenon between two polymers was investigated. From scanning electron microscopic studies, it appeared that the thickness variation of the active layer, by alternating self-assembly of cationic and anionic polymers on porous supporting membranes, highly depends on the chitosan concentration and SA content in the dipping solution during PIC membrane formation. The results are attributed to the fact that the chitosan molecules diffuse from the liquid solution into the SA matrix and incorporate with sodium alginate molecules. In particular, the morphology of PIC membranes was determined by the strong physical transition status of pure SA membrane, and the overall structural changes were affected by an electrostatic interaction between the particles in the SA membranes and the chitosan molecules. The morphological changes influenced the mechanical properties of PIC membranes. From FTIR and XRD results, it was observed that the amorphous state of PIC membranes increased as a function of polymer contents, although the chemical differences of PIC were very small.

REFERENCES

1. Neel, J. in Introduction to Pervaporation; Huang, R. Y. M., Ed.; Pervaporation Membrane Separation Processes; Elsevier: New York, 1991; p 42.
2. Peniche-Covas, C.; Argüelles-Monal, W.; Román, J. S. Polym Int 1995, 38, 45.
3. Ageev, E. P.; Kotova, S. L.; Skoikova, E. E.; Zezin, A. B. Polym Sci Ser A 1996, 38, 202.
4. Nam, S. Y.; Lee, Y. M. J Membr Sci 1997, 135, 161.
5. Decher, G.; Schmitt, J. Prog Colloid Polym Sci 1992, 89, 160.
6. Stoeve, G.; Vasquez, V.; Coelho, M. A. N.; Rabolt, J. F. Thin Solid Films 1996, 284, 708.
7. Grasdalen, H.; Larsen, B., Smidsrød, O. Carbohydr Res 1981, 89, 179.
8. Martinsen, A.; Skjäk-Braek, G.; Smidsrød, O. Biotechnol Bioeng 1989, 33, 79.
9. Goosen, M. F. A., Ed. Applications of Chitin and Chitosan; Technomic Publishing: Lancaster, PA, 1998.
10. Grant, G. T.; Morris, E. R.; Rees, D. A.; Smith, P. J. C.; Thom, D. FEBS Lett 1973, 32, 195.
11. Yin, Y. J.; Yao, K. D.; Cheng, G. X.; Ma, J. B. Polym Int 1999, 48, 429.
12. Sartori, C.; Finch, D. S.; Ralph, B.; Gilding, K. Polymer 1997, 38, 43.
13. Zang, S.; Gonsalves, K. E. J Appl Polym Sci 1995, 56, 687.
14. Salmon, S.; Hudson, S. M. Rev Macromol Chem Phys 1997, C37, 199.
15. Kim, J. H.; Lee, Y. M. Polymer 1993, 34, 1952.